

# DF-GAN: A Simple and Effective Baseline for Text-to-Image Synthesis

Ming Tao<sup>1</sup> Hao Tang<sup>2</sup> Fei Wu<sup>1</sup> Xiaoyuan Jing<sup>3</sup> Bing-Kun Bao<sup>1\*</sup> Changsheng Xu<sup>4,5,6</sup>  
<sup>1</sup>Nanjing University of Posts and Telecommunications <sup>2</sup>CVL, ETH Zürich <sup>3</sup>Wuhan University  
<sup>4</sup>Peng Cheng Laboratory <sup>5</sup>University of Chinese Academy of Sciences  
<sup>6</sup>NLPR, Institute of Automation, CAS

bingkunbao@njupt.edu.cn

## Abstract

Synthesizing high-quality realistic images from text descriptions is a challenging task. Existing text-to-image Generative Adversarial Networks generally employ a stacked architecture as the backbone yet still remain three flaws. First, the stacked architecture introduces the entanglements between generators of different image scales. Second, existing studies prefer to apply and fix extra networks in adversarial learning for text-image semantic consistency, which limits the supervision capability of these networks. Third, the cross-modal attention-based text-image fusion that widely adopted by previous works is limited on several special image scales because of the computational cost. To these ends, we propose a simpler but more effective Deep Fusion Generative Adversarial Networks (DF-GAN). To be specific, we propose: (i) a novel one-stage text-to-image backbone that directly synthesizes high-resolution images without entanglements between different generators, (ii) a novel Target-Aware Discriminator composed of Matching-Aware Gradient Penalty and One-Way Output, which enhances the text-image semantic consistency without introducing extra networks, (iii) a novel deep text-image fusion block, which deepens the fusion process to make a full fusion between text and visual features. Compared with current state-of-the-art methods, our proposed DF-GAN is simpler but more efficient to synthesize realistic and text-matching images and achieves better performance on widely used datasets. Code is available at <https://github.com/tobran/DF-GAN>.

## 1. Introduction

The last few years have witnessed the great success of Generative Adversarial Networks (GANs) [8] for a variety of applications [4, 27, 48]. Among them, text-to-image synthesis is one of the most important applications of GANs.

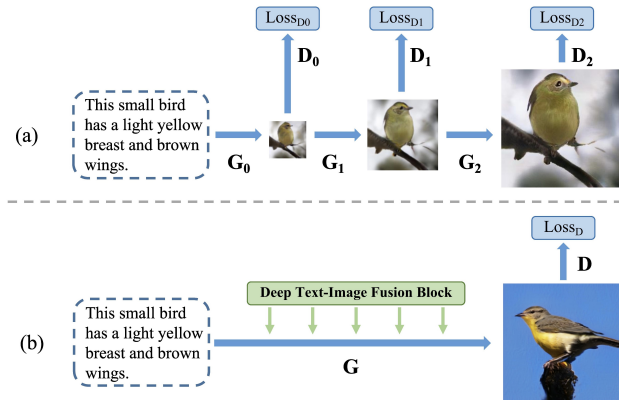


Figure 1. (a) Existing text-to-image models stack multiple generators to generate high-resolution images. (b) Our proposed DF-GAN generates high-quality images directly and fuses the text and image features deeply by our deep text-image fusion blocks.

It aims to generate realistic and text-consistent images from the given natural language descriptions. Due to its practical value, text-to-image synthesis has become an active research area recently [3, 9, 13, 19–21, 32, 33, 35, 51, 53, 60].

Two major challenges for text-to-image synthesis are the authenticity of the generated image, and the semantic consistency between the given text and the generated image. Due to the instability of the GAN model, most recent models adopt the stacked architecture [56, 57] as the backbone to generate high-resolution images. They employ cross-modal attention to fuse text and image features [37, 50, 56, 57, 60] and then introduce DAMSM network [50], cycle consistency [33], or Siamese network [51] to ensure the text-image semantic consistency by extra networks.

Although impressive results have been presented by previous works [9, 19, 21, 32, 33, 51, 60], there still remain three problems. First, the stacked architecture [56] introduces entanglements between different generators, and this makes the final refined images look like a simple combination of fuzzy shape and some details. As shown in Figure 1(a), the final refined image has a fuzzy shape synthesized by  $G_0$ , coarse attributes (e.g., eye and beak) synthesized by

\*Corresponding Author

$G_1$ , and fine-grained details (e.g., eye reflection) added by  $G_2$ . The final synthesized image looks like a simple combination of visual features from different image scales. Second, existing studies usually fix the extra networks [33, 50] during the adversarial training, making these networks easily fooled by the generator to synthesize adversarial features [30, 52], thereby weakening their supervision power on semantic consistency. Third, cross-modal attention [50] can not make full use of text information. They can only be applied two times on  $64 \times 64$  and  $128 \times 128$  image features due to its high computational cost. It limits the effectiveness of the text-image fusion process and makes the model hard to extend to higher-resolution image synthesis.

To address the above issues, we propose a novel text-to-image generation method named Deep Fusion Generative Adversarial Network (DF-GAN). For the first issue, we replace the stacked backbone with a one-stage backbone. It is composed of hinge loss [54] and residual networks [11] which stabilizes the GAN training process to synthesize high-resolution images directly. Since there is only one generator in the one-stage backbone, it avoids the entanglements between different generators.

For the second issue, we design a Target-Aware Discriminator composed of Matching-Aware Gradient Penalty (MA-GP) and One-Way Output to enhance the text-image semantic consistency. MA-GP is a regularization strategy on the discriminator. It pursues the gradient of discriminator on target data (real and text-matching image) to be zero. Thereby, the MA-GP constructs a smooth loss surface at real and matching data points which further promotes the generator to synthesize text-matching images. Moreover, considering that the previous Two-Way Output slows down the convergence process of the generator under MA-GP, we replace it with a more effective One-Way Output.

For the third issue, we propose a Deep text-image Fusion Block (DFBlock) to fuse the text information into image features more effectively. The DFBlock consists of several Affine Transformations [31]. The Affine Transformation is a lightweight module that manipulates the visual feature maps through channel-wise scaling and shifting operation. Stacking multiple DFBlocks at all image scales deepens the text-image fusion process and makes a full fusion between text and visual features.

Overall, our contributions can be summarized as follows:

- We propose a novel one-stage text-to-image backbone that can synthesize high-resolution images directly without entanglements between different generators.
- We propose a novel Target-Aware Discriminator composed of Matching-Aware Gradient Penalty (MA-GP) and One-Way Output. It significantly enhances the text-image semantic consistency without introducing extra networks.

- We propose a novel Deep text-image Fusion Block (DFBlock), which fully fuses text and visual features more effectively and deeply.
- Extensive qualitative and quantitative experiments on two challenging datasets demonstrate that the proposed DF-GAN outperforms existing state-of-the-art text-to-image models.

## 2. Related Work

Generative Adversarial Networks (GANs) [8] are an attractive framework that can be used to mimic complex real-world distributions by solving a min-max optimization problem between a generator and discriminator [16, 17, 43, 54]. For instance, Reed *et al.* first applied the conditional GAN to generate plausible images from text descriptions [37, 38]. StackGAN [56, 57] generates high-resolution images by stacking multiple generators and discriminators and provides the text information to the generator by concatenating text vectors as well as the input noises. Next, AttnGAN [50] introduces the cross-modal attention mechanism to help the generator synthesize images with more details. MirrorGAN [33] regenerates text descriptions from generated images for text-image semantic consistency [59]. SD-GAN [51] employs the Siamese structure [45, 46] to distill the semantic commons from texts for image generation consistency. DM-GAN [60] introduces the Memory Network [10, 49] to refine fuzzy image contents when the initial images are not well generated in stacked architecture. Recently, some large transformer-based text-to-image methods [7, 24, 35] show excellent performance on complex image synthesis. They tokenize the images and take the image tokens and word tokens to make auto-regressive training by a unidirectional Transformer [2, 34].

Our DF-GAN is much different from previous methods. First, it generates high-resolution images directly by a one-stage backbone. Second, it adopts a Target-Aware Discriminator to enhance text-image semantic consistency without introducing extra networks. Third, it fuses text and image features more deeply and effectively through a sequence of DFBlocks. Compared with previous models, our DF-GAN is much simpler but more effective in synthesizing realistic and text-matching images.

## 3. The Proposed DF-GAN

In this paper, we propose a simple model for text-to-image synthesis named Deep Fusion GAN (DF-GAN). To synthesize more realistic and text-matching images, we propose: (i) a novel one-stage text-to-image backbone that can synthesize high-resolution images directly without visual feature entanglements. (ii) a novel Target-Aware Discriminator composed of Matching-Aware Gradient Penalty

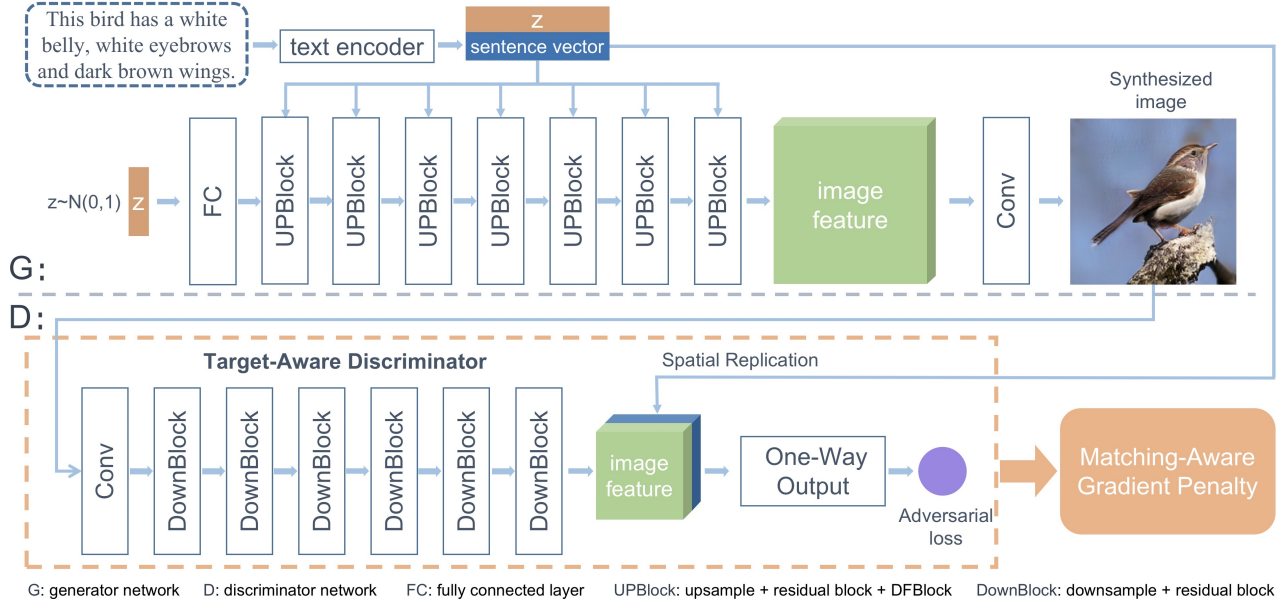


Figure 2. The architecture of the proposed DF-GAN for text-to-image synthesis. DF-GAN generates high-resolution images directly by one pair of generator and discriminator and fuses the text information and visual feature maps through multiple Deep text-image Fusion Blocks (DFBlock) in UPBlocks. Armed with Matching-Aware Gradient Penalty (MA-GP) and One-Way Output, our model can synthesize more realistic and text-matching images.

(MA-GP) and One-Way Output, which enhances the text-image semantic consistency without introducing extra networks. (iii) a novel Deep text-image Fusion Block (DF-Block), which more fully fuses text and visual features.

### 3.1. Model Overview

The proposed DF-GAN is composed of a generator, a discriminator, and a pre-trained text encoder as shown in Figure 2. The generator has two inputs, a sentence vector encoded by text encoder and a noise vector sampled from the Gaussian distribution to ensure the diversity of the generated images. The noise vector is first fed into a fully connected layer and reshaped. We then apply a series of UP-Blocks to upsample the image features. The UPBlock is composed of an upsample layer, a residual block, and DF-Blocks to fuse the text and image features during the image generation process. Finally, a convolution layer converts image features into images.

The discriminator converts images into image features through a series of DownBlocks. Then the sentence vector will be replicated and concatenated with image features. An adversarial loss will be predicted to evaluate the visual realism and semantic consistency of inputs. By distinguishing generated images from real samples, the discriminator promotes the generator to synthesize images with higher quality and text-image semantic consistency.

The text encoder is a bi-directional Long Short-Term Memory (LSTM) [41] that extracts semantic vectors from the text description. We directly use the pre-trained model provided by AttnGAN [50].

### 3.2. One-Stage Text-to-Image Backbone

Since the instability of the GAN model, previous text-to-image GANs usually employ stacked architecture [56,57] to generate high-resolution images from low-resolution ones. However, the stacked architecture introduces entanglements between different generators, and it makes the final refined images look like a simple combination of fuzzy shape and some details (see Figure 1(a)).

Inspired by recent studies on unconditional image generation [23,54], we propose a one-stage text-to-image backbone that can synthesize high-resolution images directly by a single pair of generator and discriminator. We employ the hinge loss [23] to stabilize the adversarial training process. Since there is only one generator in the one-stage backbone, it avoids the entanglements between different generators. As the single generator in our one-stage framework needs to synthesize high-resolution images from noise vectors directly, it must contain more layers than previous generators in stacked architecture. To train these layers effectively, we introduce residual networks [11] to stabilize the training of deeper networks. The formulation of our one-stage method with hinge loss [23] is as follows:

$$\begin{aligned}
 L_D &= -\mathbb{E}_{x \sim \mathbb{P}_r} [\min(0, -1 + D(x, e))] \\
 &\quad - (1/2) \mathbb{E}_{G(z) \sim \mathbb{P}_g} [\min(0, -1 - D(G(z), e))] \\
 &\quad - (1/2) \mathbb{E}_{x \sim \mathbb{P}_{mis}} [\min(0, -1 - D(x, e))] \\
 L_G &= -\mathbb{E}_{G(z) \sim \mathbb{P}_g} [D(G(z), e)]
 \end{aligned} \tag{1}$$

where  $z$  is the noise vector sampled from Gaussian distribution;  $e$  is the sentence vector;  $\mathbb{P}_g$ ,  $\mathbb{P}_r$ ,  $\mathbb{P}_{mis}$  denote the

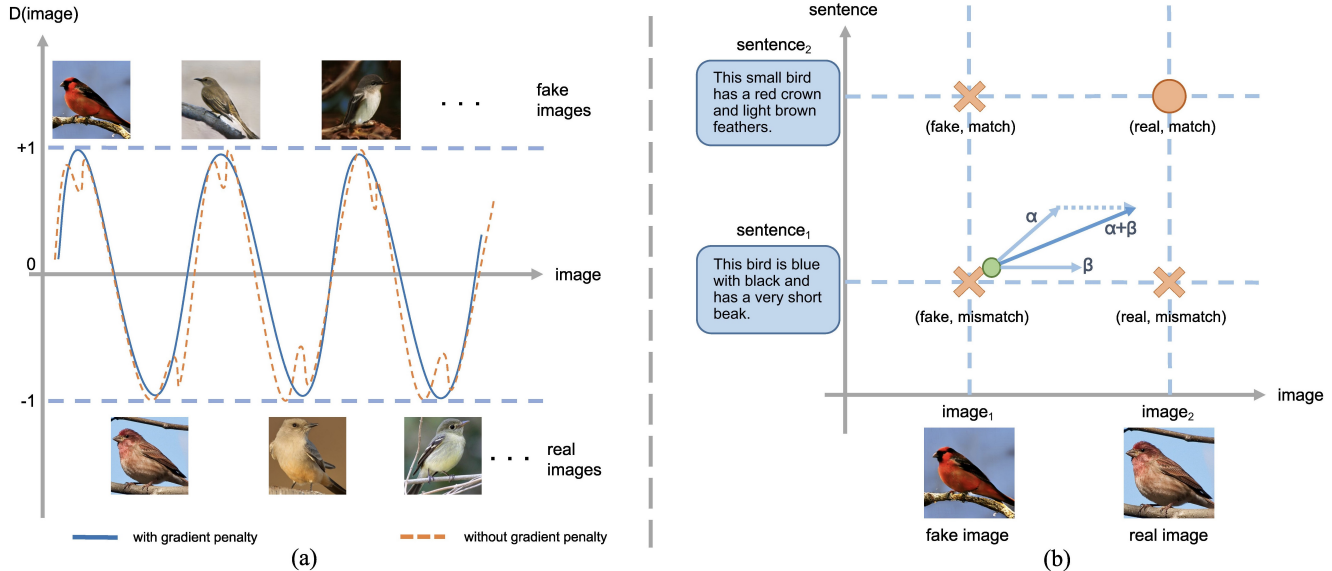


Figure 3. (a) A comparison of loss landscape before and after applying gradient penalty. The gradient penalty smooths the discriminator loss surface which is helpful for generator convergence. (b) A diagram of MA-GP. The data point (real, match) should be applied MA-GP.

synthetic data distribution, real data distribution, and mismatching data distribution, respectively.

### 3.3. Target-Aware Discriminator

In this section, we detailed the proposed Target-Aware Discriminator, which is composed of Matching-Aware Gradient Penalty (MA-GP) and One-Way Output. The Target-Aware Discriminator promotes the generator to synthesize more realistic and text-image semantic-consistent images.

#### 3.3.1 Matching-Aware Gradient Penalty

The Matching-Aware zero-centered Gradient Penalty (MA-GP) is our newly designed strategy to enhance text-image semantic consistency. In this subsection, we first show the unconditional gradient penalty [28] from a novel and clear perspective, then extend it to our MA-GP for the text-to-image generation task.

As shown in Figure 3(a), in unconditional image generation, the target data (real images) correspond to a low discriminator loss. Correspondingly, the synthetic images correspond to a high discriminator loss. The hinge loss limits the range of discriminator loss between -1 and 1. The gradient penalty on real data will reduce the gradient of the real data point and its vicinity. The surface of the loss function around the real data point is then smoothed which is helpful for the synthetic data point to converge to the real data point.

Based on the above analysis, we find that the gradient penalty on target data constructs a better loss landscape to help the generator converge. By leveraging the view into the text-to-image generation. As shown in Figure 3(b), in text-to-image generation, the discriminator ob-

serves four kinds of inputs: synthetic images with matching text (fake, match), synthetic images with mismatched text (fake, mismatch), real images with matching text (real, match), real images with mismatched text (real, mismatch). For text-visual semantic consistency, we tend to apply gradient penalty on the text-matching real data, the target of text-to-image synthesis. Therefore, in MA-GP, the gradient penalty should be applied on real images with matching text. The whole formulation of our model with MA-GP is as follows:

$$\begin{aligned}
 L_D &= -\mathbb{E}_{x \sim \mathbb{P}_r}[\min(0, -1 + D(x, e))] \\
 &\quad - (1/2)\mathbb{E}_{G(z) \sim \mathbb{P}_g}[\min(0, -1 - D(G(z), e))] \\
 &\quad - (1/2)\mathbb{E}_{x \sim \mathbb{P}_{mis}}[\min(0, -1 - D(x, e))] \quad (2) \\
 &\quad + k\mathbb{E}_{x \sim \mathbb{P}_r}[(\|\nabla_x D(x, e)\| + \|\nabla_e D(x, e)\|)^p] \\
 L_G &= -\mathbb{E}_{G(z) \sim \mathbb{P}_g}[D(G(z), e)]
 \end{aligned}$$

where  $k$  and  $p$  are two hyper-parameters to balance the effectiveness of gradient penalty.

By using the MA-GP loss as a regularization on the discriminator, our model can better converge to the text-matching real data, therefore synthesizing more text-matching images. Besides, since the discriminator is jointly trained in our network, it prevents the generator from synthesizing adversarial features of the fixed extra network. Moreover, since MA-GP does not incorporate any extra networks for text-image consistency and the gradients are already computed by back propagation process, the only computation introduced by our proposed MA-GP is the gradient summation, which is more computational friendly than extra networks.

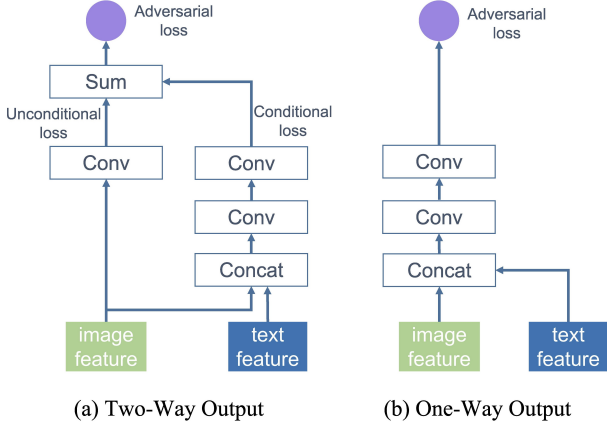


Figure 4. Comparison between Two-Way Output and our One-Way Output. (a) The Two-Way Output predicts conditional loss and unconditional loss and sums them up as the final adversarial loss. (b) Our One-Way Output predicts the whole adversarial loss directly.

### 3.3.2 One-Way Output

In the previous text-to-image GANs [50,56,57], image features extracted by discriminator are usually used in two ways (Figure 4(a)): one determines whether the image is real or fake, the other concatenates the image feature and sentence vector to evaluate text-image semantic consistency. Correspondingly, the unconditional loss and the conditional loss are computed in these models.

However, it is shown that the Two-Way Output weakens the effectiveness of MA-GP and slows down the convergence of the generator. Concretely, as depicted in Figure 3(b), the conditional loss gives a gradient  $\alpha$  pointing to the real and matching inputs after back propagation, while the unconditional loss gives a gradient  $\beta$  only pointing to the real images. However, the direction of the final gradient which just simply sums up  $\alpha$  and  $\beta$  does not point to the real and matching data points as we expected. Since the target of the generator is to synthesize real and text-matching images, the final gradient with deviation cannot well achieve text-image semantic consistency and slows down the convergence process of the generator.

Therefore, we propose the One-Way Output for text-to-image synthesis. As shown in Figure 4(b), our discriminator concatenates the image feature and sentence vector, then outputs only one adversarial loss through two convolution layers. Through the One-Way Output, we are able to make the single gradient  $\alpha$  pointed to the target data points (real and match) directly, which optimize and accelerate the convergence of the generator.

By combining the MA-GP and the One-Way Output, our Target-Aware Discriminator can guide the generator to synthesize more real and text-matching images.

### 3.4. Efficient Text-Image Fusion

To fuse text and image features efficiently, we propose a novel Deep text-image Fusion Block (DFBlock). Compared with previous text-image fusion modules, our DFBlock deepens the text-image fusion process to make a full text-image fusion.

As shown in Figure 2, the generator of our DF-GAN consists of 7 UPBlocks. A UPBlock contains two Text-Image Fusion blocks. To fully utilize the text information in fusion, we propose the Deep text-image Fusion Block (DFBlock) which stacks multiple Affine Transformations and ReLU layers in Fusion Block. For Affine transformation, as shown in Figure 5(c), we adopt two MLPs (Multilayer Perceptron) to predict the language-conditioned channel-wise scaling parameters  $\gamma$  and shifting parameters  $\theta$  from sentence vector  $e$ , respectively:

$$\gamma = MLP_1(e), \quad \theta = MLP_2(e). \quad (3)$$

For a given input feature map  $X \in \mathbb{R}^{B \times C \times H \times W}$ , we first conduct the channel-wise scaling operation on  $X$  with the scaling parameter  $\gamma$ , then apply the channel-wise shifting operation with the shifting parameter  $\theta$ . Such a process can be expressed as follows:

$$AFF(x_i|e) = \gamma_i \cdot x_i + \theta_i, \quad (4)$$

where  $AFF$  denotes the Affine Transformation;  $x_i$  is the  $i^{th}$  channel of visual feature maps;  $e$  is the sentence vector;  $\gamma_i$  and  $\theta_i$  are scaling parameter and shifting parameter for the  $i^{th}$  channel of visual feature maps.

The Affine layer expands the conditional representation space of the generator. However, the Affine transformation is a linear transformation for each channel. It limits the effectiveness of text-image fusion process. Thereby, we add a ReLU layer between two Affine layers which brings the nonlinearity into the fusion process. It enlarges the conditional representation space compared with only one Affine layer. A larger representation space is helpful for the generator to map different images to different representations according to text descriptions.

Our DFBlock is partly inspired by Conditional Batch Normalization (CBN) [5] and Adaptive Instance Normalization (AdaIN) [14,16] which contain the Affine transformation. However, both CBN and AdaIN employ normalization layers [15,44] which transform the feature maps into the normal distribution. It generates an opposite effect to the Affine Transformation which is expected to increase the distance between different samples. It is then unhelpful for the conditional generation process. To this end, we remove the normalization process. Furthermore, our DFBlock deepens the text-image fusion process. We stack multiple Affine layers and add a ReLU layer between. It promotes the diversity of visual features and enlarges the representation spaces to

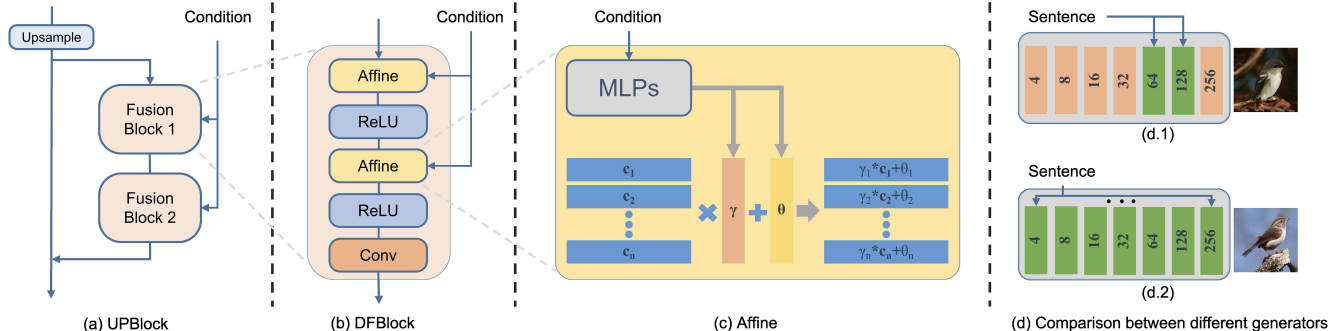


Figure 5. (a) A typical UPBlock in the generator network. The UPBlock upsamples the image features and fuses text and image features by two Fusion Blocks. (b) The DFBlock consists of two Affine layers, two ReLU activation layers, and a Convolution layer. (c) The illustration of the Affine Transformation. (d) Comparison between (d.1) the generator with cross-modal attention [50, 60] and (d.2) our generator with DFBlock.

represent different visual features according to different text descriptions.

With the deepening of the fusion process, the DFBlock brings two main benefits for text-to-image generation: First, it makes the generator more fully exploit the text information when fusing text and image features. Second, deepening the fusion process enlarges the representation space of the fusion module, which is beneficial to generate semantic consistent images from different text descriptions.

Furthermore, compared with previous text-to-image GANs [50, 56, 57, 60], the proposed DFBlock makes our model no longer consider the limitation from image scales when fusing the text and image features. This is because existing text-to-image GANs generally employ the cross-modal attention mechanism which suffers a rapid growth of computation cost along with the increase of image size.

## 4. Experiments

In this section, we first introduce the datasets, training details, and evaluation metrics used in our experiments, then evaluate DF-GAN and its variants quantitatively and qualitatively.

**Datasets.** We follow previous work [33, 50, 51, 56, 57, 60] and evaluate the proposed model on two challenging datasets, i.e., CUB bird [47] and COCO [25]. The CUB dataset contains 11,788 images belonging to 200 bird species. Each bird image has ten language descriptions. The COCO dataset contains 80k images for training and 40k images for testing. Each image in this dataset has five language descriptions.

**Training Details.** We optimize our network using Adam [18] with  $\beta_1=0.0$  and  $\beta_2=0.9$ . The learning rate is set to 0.0001 for the generator and 0.0004 for the discriminator according to Two Timescale Update Rule (TTUR) [12].

**Evaluation Details.** Following previous works [50, 60], we choose the Inception Score (IS) [40] and Fréchet Inception Distance (FID) [12] to evaluate the performance of our net-

work. Specifically, IS computes the Kullback-Leibler (KL) divergence between a conditional distribution and marginal distribution. Higher IS means higher quality of the generated images, and each image clearly belongs to a specific class. FID [12] computes the Fréchet distance between the distribution of the synthetic images and real-world images in the feature space of a pre-trained Inception v3 network. Contrary to IS, more realistic images have a lower FID. To compute both IS and FID, each model generates 30,000 images ( $256 \times 256$  resolution) from text descriptions randomly selected from the test dataset.

As stated in the recent works [21, 58], the IS cannot evaluate the image quality well on the COCO dataset, which also exists in our proposed method. Moreover, we find that some GAN-based models [50, 60] achieve significant higher IS than Transformer-based large text-to-image models [7, 35] on the COCO dataset, but the visual quality of synthesized images is obviously lower than Transformer-based models [7, 35]. Thus, we do not compare IS on the COCO dataset. In contrast, FID is more robust and aligns human qualitative evaluation on the COCO dataset.

Moreover, we evaluate the number of parameters (NoP) to compare the model size with current methods.

### 4.1. Quantitative Evaluation

We compare the proposed method with several state-of-the-art methods, including StackGAN [56], StackGAN++ [57], AttnGAN [50], MirrorGAN [33], SD-GAN [51], and DM-GAN [60], which have achieved the remarkable success of text-to-image synthesis by using stacked structures. We also compared with more recent models [22, 26, 39, 55]. It should be pointed that recent models always use extra knowledge or supervisions. For example, CPGAN [22] uses the extra pretrained YOLO-V3 [36], XMC-GAN [55] uses the extra pretrained VGG-19 [42] and Bert [6], DAE-GAN [39] uses extra NLTK POS tagging and manually designs rules for different datasets, and TIME [26] uses extra 2-D positional encoding.



Figure 6. Examples of images synthesized by AttnGAN [50], DM-GAN [60], and our proposed DF-GAN conditioned on text descriptions from the test set of COCO and CUB datasets.

Table 1. The results of IS, FID and NoP compared with the state-of-the-art methods on the test set of CUB and COCO.

Model	CUB		COCO	
	IS $\uparrow$	FID $\downarrow$	FID $\downarrow$	NoP $\downarrow$
StackGAN [56]	3.70	-	-	-
StackGAN++ [57]	3.84	-	-	-
AttnGAN [50]	4.36	23.98	35.49	230M
MirrorGAN [33]	4.56	18.34	34.71	-
SD-GAN [51]	4.67	-	-	-
DM-GAN [60]	4.75	16.09	32.64	46M
CPGAN [22]	-	-	55.80	318M
XMC-GAN [55]	-	-	9.30	166M
DAE-GAN [39]	4.42	15.19	28.12	98M
TIME [26]	4.91	14.30	31.14	120M
DF-GAN (Ours)	5.10	14.81	19.32	19M

As shown in Table 1, compared with other leading models, our DF-GAN has a significant smaller Number of Parameters (NoP) but still achieves a competitive performance. Compared with AttnGAN [50] which employs cross-modal attention to fuse text and image features, our DF-GAN improves the IS metric from 4.36 to 5.10 and decreases the FID metric from 23.98 to 14.81 on the CUB dataset. And our DF-GAN decreases FID from 35.49 to 19.32 on the COCO dataset. Compared with MirrorGAN [33] and SD-GAN [51] which employ cycle consistency and Siamese network to ensure text-image semantic consistency, our DF-GAN improves IS from 4.56 and 4.67 to 5.10, respectively on the CUB dataset. Compared with DM-GAN [60] which introduces Memory Network to refine fuzzy image contents, our model also improves IS from 4.75 to 5.10 and decreases FID from 16.09 to 14.81 on CUB,

and also decreases FID from 32.64 to 19.32 on the COCO. Moreover, compared with recent models which introduce extra knowledge, our DF-GAN still achieves a competitive performance. The quantitative comparisons prove that our model is much simpler but more effective.

## 4.2. Qualitative Evaluation

We also compare the visualization results synthesized by AttnGAN [50], DM-GAN [60], and the proposed DF-GAN.

It can be seen that images synthesized by AttnGAN [50] and DM-GAN [60] in Figure 6 look like a simple combination of fuzzy shape and some visual details (1<sup>st</sup>, 3<sup>rd</sup>, 5<sup>th</sup>, 7<sup>th</sup>, and 8<sup>th</sup> columns). As shown in the 5<sup>th</sup>, 7<sup>th</sup>, and 8<sup>th</sup> columns, the birds synthesized by AttnGAN [50] and DM-GAN [60] contain wrong shapes. Moreover, the images synthesized by our DF-GAN have better object shapes and realistic fine-grained details (e.g., 1<sup>st</sup>, 3<sup>rd</sup>, 7<sup>th</sup>, and 8<sup>th</sup> columns). Besides, the posture of the bird in our DF-GAN result is also more natural (e.g., 7<sup>th</sup> and 8<sup>th</sup> columns).

Comparing the text-image semantic consistency with other models, we find that our DF-GAN can also capture more fine-grained details in text descriptions. For example, as the results shown in 1<sup>st</sup>, 2<sup>th</sup>, 6<sup>th</sup> columns in Figure 6, other models cannot synthesize the “holding ski poles”, “train track”, and “a black stripe by its eyes” described in the text well, but the proposed DF-GAN can synthesize them more correctly.

## 4.3. Ablation Study

In this section, we conduct ablation studies on the testing set of the CUB dataset to verify the effectiveness of each component in the proposed DF-GAN. The com-

Table 2. The performance of different components of our model on the test set of CUB.

Architecture	IS $\uparrow$	FID $\downarrow$	SC $\uparrow$
Baseline	3.96	51.34	-
OS-B	4.11	43.45	1.46
OS-B w/ DAMSM	4.28	36.72	1.79
OS-B w/ MA-GP	4.46	32.52	3.55
OS-B w/ MA-GP w/ OW-O	<b>4.57</b>	<b>23.16</b>	<b>4.61</b>

ponents include One-Stage text-to-image Backbone (OS-B), Matching-Aware Gradient Penalty (MA-GP), One-Way Output (OW-O), Deep text-image Fusion Block (DFBlock). We also compare our Target-Aware Discriminator with Deep Attentional Multimodal Similarity Model (DAMSM) which is an extra network widely employed in current models [50, 51, 60]. We first evaluate the effectiveness of OS-B, MA-GP, and OW-O. We conducted a user study to evaluate the text-image semantic consistency (SC), and we asked ten users to score the 100 randomly synthesized images with text descriptions. The scores range from 1 (worst) to 5 (best). The results on the CUB dataset are shown in Table 2.

**Baseline.** Our baseline employs stacked framework and Two-Way Output with the same Adversarial loss as StackGAN [56]. In baseline, the sentence vector is naively concatenated to the input noise and intermediate feature maps.

**Effect of One-Stage Backbone.** Our proposed OS-B improves IS from 3.96 to 4.11 and decreases FID from 43.45 to 32.52. The results demonstrate that our one-stage backbone is more effective than stacked architecture.

**Effect of MA-GP.** Armed with MA-GP, the model further improves IS to 4.46, SC to 3.55, and decreases FID to 32.52 significantly. It demonstrates that the proposed MA-GP can promote the generator to synthesize more realistic and text-image semantic consistent images.

**Effect of One-Way Output.** The proposed OW-O also improves IS from 4.46 to 4.57, SC from 3.55 to 4.61, and decreases FID from 32.52 to 23.16. It also demonstrates that the One-Way Output is more effective than a Two-Way Output in the text-to-image generation task.

**Effect of Target-Aware Discriminator.** Compared with DAMSM, our proposed Target-Aware Discriminator composed of MA-GP and OW-O improves IS from 4.28 to 4.57, SC from 1.79 to 4.61, and decreases FID from 36.72 to 23.16. The results demonstrate that our Target-Aware Discriminator is superior to extra networks.

**Effect of DFBlock.** We compare our DFBlock with CBN [1, 5, 29], AdaIN [16] and AFFBlock. The AFFBlock employs one Affine Transformation layer to fuse text and image features. MA-GP GAN is the model that employs One-Stage text-to-image Backbone, Matching-Aware Gradient Penalty, and One-Way Output. From the results in Table 3, we find that, compared with other fusion methods, concatenation cannot efficiently fuse text and image fea-

Table 3. The performance of MA-GP GAN with different modules on the test set of CUB.

Architecture	IS $\uparrow$	FID $\downarrow$
MA-GP GAN w/ Concat	4.57	23.16
MA-GP GAN w/ CBN	4.81	18.56
MA-GP GAN w/ AdaIN	4.85	17.52
MA-GP GAN w/ AFFBLK	4.87	17.43
MA-GP GAN w/ DFBLK (DF-GAN)	<b>5.10</b>	<b>14.81</b>

tures. The comparison among CBN, AdaIN, and AFFBlock proves that Normalization is not essential in Fusion Block, and removing normalization even slightly improves the results. The comparison between DFBlock and AFFBlock demonstrates the effectiveness of deepening the text-image fusion process. In sum, the comparison results prove the effectiveness of our proposed DFBlock.

#### 4.4. Limitations

Although DF-GAN shows superiority in text-to-image synthesis, some limitations must be taken into consideration in future studies. First, our model only introduces the sentence-level text information, which limits the ability of fine-grained visual feature synthesis. Second, introducing pre-trained large language models [6, 34] to provide additional knowledge may further improve the performance. We will try to address these limitations in our future work.

## 5. Conclusion and Future Work

In this paper, we propose a novel DF-GAN for the text-to-image generation tasks. We present a one-stage text-to-image Backbone that can synthesize high-resolution images directly without entanglements between different generators. We also propose a novel Target-Aware Discriminator composed of Matching-Aware Gradient Penalty (MA-GP) and One-Way Output. It can further enhance the text-image semantic consistency without introducing extra networks. Besides, we introduce a novel Deep text-image Fusion Block (DFBlock) which fully fuses text and image features more effectively and deeply. Extensive experiment results demonstrate that our proposed DF-GAN significantly outperforms current state-of-the-art models on the CUB dataset and more challenging COCO dataset.

## Acknowledgment

This work was supported by National Key Research and Development Project (No.2020AAA0106200), the National Nature Science Foundation of China under Grants (No.61936005, 61872424, 62076139, 62176069 and 61933013), the Natural Science Foundation of Jiangsu Province (Grants No.BK20200037 and BK20210595), and the Open Research Project of Zhejiang Lab (No.2021KF0AB05).



## References

- [1] Andrew Brock, Jeff Donahue, and Karen Simonyan. Large scale gan training for high fidelity natural image synthesis. In *International Conference on Learning Representations*, 2019. 8
- [2] Tom B Brown, Benjamin Mann, Nick Ryder, Melanie Subbiah, Jared Kaplan, Prafulla Dhariwal, Arvind Neelakantan, Pranav Shyam, Girish Sastry, Amanda Askell, et al. Language models are few-shot learners. *arXiv preprint arXiv:2005.14165*, 2020. 2
- [3] Jun Cheng, Fuxiang Wu, Yanling Tian, Lei Wang, and Dapeng Tao. Rifegan: Rich feature generation for text-to-image synthesis from prior knowledge. In *Proceedings of the IEEE/CVF Conference on Computer Vision and Pattern Recognition*, pages 10911–10920, 2020. 1
- [4] Wen-Huang Cheng, Sijie Song, Chieh-Yun Chen, Shintami Chusnul Hidayati, and Jiaying Liu. Fashion meets computer vision: A survey. *ACM Computing Surveys (CSUR)*, 54(4):1–41, 2021. 1
- [5] Harm De Vries, Florian Strub, Jérémie Mary, Hugo Larochelle, Olivier Pietquin, and Aaron C Courville. Modulating early visual processing by language. In *Advances in Neural Information Processing Systems*, pages 6594–6604, 2017. 5, 8
- [6] Jacob Devlin, Ming-Wei Chang, Kenton Lee, and Kristina Toutanova. Bert: Pre-training of deep bidirectional transformers for language understanding. *arXiv preprint arXiv:1810.04805*, 2018. 6, 8
- [7] Ming Ding, Zhuoyi Yang, Wenyi Hong, Wendi Zheng, Chang Zhou, Da Yin, Junyang Lin, Xu Zou, Zhou Shao, Hongxia Yang, et al. Cogview: Mastering text-to-image generation via transformers. *arXiv preprint arXiv:2105.13290*, 2021. 2, 6
- [8] Ian Goodfellow, Jean Pouget-Abadie, Mehdi Mirza, Bing Xu, David Warde-Farley, Sherjil Ozair, Aaron Courville, and Yoshua Bengio. Generative adversarial nets. In *Advances in Neural Information Processing Systems*, pages 2672–2680, 2014. 1, 2
- [9] Yuchuan Gou, Qiancheng Wu, Minghao Li, Bo Gong, and Mei Han. Segattngan: Text to image generation with segmentation attention. *arXiv preprint arXiv:2005.12444*, 2020. 1
- [10] Caglar Gulcehre, Sarath Chandar, Kyunghyun Cho, and Yoshua Bengio. Dynamic neural turing machine with continuous and discrete addressing schemes. *Neural computation*, 30(4):857–884, 2018. 2
- [11] Kaiming He, Xiangyu Zhang, Shaoqing Ren, and Jian Sun. Deep residual learning for image recognition. In *Proceedings of the IEEE conference on computer vision and pattern recognition*, pages 770–778, 2016. 2, 3
- [12] Martin Heusel, Hubert Ramsauer, Thomas Unterthiner, Bernhard Nessler, and Sepp Hochreiter. Gans trained by a two time-scale update rule converge to a local nash equilibrium. In *Advances in neural information processing systems*, pages 6626–6637, 2017. 6
- [13] Seunghoon Hong, Dingdong Yang, Jongwook Choi, and Honglak Lee. Inferring semantic layout for hierarchical text-to-image synthesis. In *Proceedings of the IEEE Conference on Computer Vision and Pattern Recognition*, pages 7986–7994, 2018. 1
- [14] Xun Huang and Serge Belongie. Arbitrary style transfer in real-time with adaptive instance normalization. In *Proceedings of the IEEE International Conference on Computer Vision*, pages 1501–1510, 2017. 5
- [15] Sergey Ioffe and Christian Szegedy. Batch normalization: Accelerating deep network training by reducing internal covariate shift. In *International Conference on Machine Learning*, 2015. 5
- [16] Tero Karras, Samuli Laine, and Timo Aila. A style-based generator architecture for generative adversarial networks. In *Proceedings of the IEEE conference on computer vision and pattern recognition*, pages 4401–4410, 2019. 2, 5, 8
- [17] Tero Karras, Samuli Laine, Miika Aittala, Janne Hellsten, Jaakko Lehtinen, and Timo Aila. Analyzing and improving the image quality of stylegan. In *Proceedings of the IEEE/CVF Conference on Computer Vision and Pattern Recognition*, pages 8110–8119, 2020. 2
- [18] Diederik P Kingma and Jimmy Ba. Adam: A method for stochastic optimization. In *International Conference on Learning Representations*, 2015. 6
- [19] Bowen Li, Xiaojuan Qi, Thomas Lukasiewicz, and Philip Torr. Controllable text-to-image generation. In *Advances in Neural Information Processing Systems*, pages 2065–2075, 2019. 1
- [20] Ruifan Li, Ning Wang, Fangxiang Feng, Guangwei Zhang, and Xiaojie Wang. Exploring global and local linguistic representation for text-to-image synthesis. *IEEE Transactions on Multimedia*, 2020. 1
- [21] Wenbo Li, Pengchuan Zhang, Lei Zhang, Qiuyuan Huang, Xiaodong He, Siwei Lyu, and Jianfeng Gao. Object-driven text-to-image synthesis via adversarial training. In *Proceedings of the IEEE Conference on Computer Vision and Pattern Recognition*, pages 12174–12182, 2019. 1, 6
- [22] Jiadong Liang, Wenjie Pei, and Feng Lu. Cpgan: Content-parsing generative adversarial networks for text-to-image synthesis. In *European Conference on Computer Vision*, pages 491–508. Springer, 2020. 6, 7
- [23] Jae Hyun Lim and Jong Chul Ye. Geometric gan. *arXiv preprint arXiv:1705.02894*, 2017. 3
- [24] Junyang Lin, Rui Men, An Yang, Chang Zhou, Ming Ding, Yichang Zhang, Peng Wang, Ang Wang, Le Jiang, Xianyan Jia, et al. M6: A chinese multimodal pretrainer. *arXiv preprint arXiv:2103.00823*, 2021. 2
- [25] Tsung-Yi Lin, Michael Maire, Serge Belongie, James Hays, Pietro Perona, Deva Ramanan, Piotr Dollár, and C Lawrence Zitnick. Microsoft coco: Common objects in context. In *European conference on computer vision*, pages 740–755. Springer, 2014. 6
- [26] Bingchen Liu, Kunpeng Song, Yizhe Zhu, Gerard de Melo, and Ahmed Elgammal. Time: text and image mutual-translation adversarial networks. *arXiv preprint arXiv:2005.13192*, 2020. 6, 7
- [27] Ming-Yu Liu, Xun Huang, Jiahui Yu, Ting-Chun Wang, and Arun Mallya. Generative adversarial networks for image and

- video synthesis: Algorithms and applications. *Proceedings of the IEEE*, 109(5):839–862, 2021. 1
- [28] Lars Mescheder, Andreas Geiger, and Sebastian Nowozin. Which training methods for gans do actually converge? In *International Conference on Machine Learning*, pages 3481–3490, 2018. 4
- [29] Takeru Miyato and Masanori Koyama. c-gans with projection discriminator. *arXiv preprint arXiv:1802.05637*, 2018. 8
- [30] Dong Huk Park, Samaneh Azadi, Xihui Liu, Trevor Darrell, and Anna Rohrbach. Benchmark for compositional text-to-image synthesis. 2021. 2
- [31] Ethan Perez, Florian Strub, Harm De Vries, Vincent Dumoulin, and Aaron Courville. Film: Visual reasoning with a general conditioning layer. In *Proceedings of the AAAI Conference on Artificial Intelligence*, volume 32, 2018. 2
- [32] Tingting Qiao, Jing Zhang, Duanqing Xu, and Dacheng Tao. Learn, imagine and create: Text-to-image generation from prior knowledge. In *Advances in Neural Information Processing Systems*, pages 887–897, 2019. 1
- [33] Tingting Qiao, Jing Zhang, Duanqing Xu, and Dacheng Tao. Mirrorgan: Learning text-to-image generation by redescription. In *Proceedings of the IEEE Conference on Computer Vision and Pattern Recognition*, pages 1505–1514, 2019. 1, 2, 6, 7
- [34] Alec Radford, Jeffrey Wu, Rewon Child, David Luan, Dario Amodei, Ilya Sutskever, et al. Language models are unsupervised multitask learners. *OpenAI blog*, 1(8):9, 2019. 2, 8
- [35] Aditya Ramesh, Mikhail Pavlov, Gabriel Goh, Scott Gray, Chelsea Voss, Alec Radford, Mark Chen, and Ilya Sutskever. Zero-shot text-to-image generation. *arXiv preprint arXiv:2102.12092*, 2021. 1, 2, 6
- [36] Joseph Redmon and Ali Farhadi. Yolov3: An incremental improvement. *arXiv preprint arXiv:1804.02767*, 2018. 6
- [37] Scott Reed, Zeynep Akata, Xinchun Yan, Lajanugen Logeswaran, Bernt Schiele, and Honglak Lee. Generative adversarial text to image synthesis. In *Proceedings of the International Conference on Machine Learning*, pages 1060–1069, 2016. 1, 2
- [38] Scott E Reed, Zeynep Akata, Santosh Mohan, Samuel Tenka, Bernt Schiele, and Honglak Lee. Learning what and where to draw. In *Advances in neural information processing systems*, pages 217–225, 2016. 2
- [39] Shulan Ruan, Yong Zhang, Kun Zhang, Yanbo Fan, Fan Tang, Qi Liu, and Enhong Chen. Dae-gan: Dynamic aspect-aware gan for text-to-image synthesis. In *Proceedings of the IEEE/CVF International Conference on Computer Vision*, pages 13960–13969, 2021. 6, 7
- [40] Tim Salimans, Ian Goodfellow, Wojciech Zaremba, Vicki Cheung, Alec Radford, and Xi Chen. Improved techniques for training gans. In *Advances in neural information processing systems*, pages 2234–2242, 2016. 6
- [41] Mike Schuster and Kuldip K Paliwal. Bidirectional recurrent neural networks. *IEEE transactions on Signal Processing*, 45(11):2673–2681, 1997. 3
- [42] Karen Simonyan and Andrew Zisserman. Very deep convolutional networks for large-scale image recognition. *arXiv preprint arXiv:1409.1556*, 2014. 6
- [43] Hao Tang, Song Bai, Li Zhang, Philip HS Torr, and Nicu Sebe. Xinggan for person image generation. In *ECCV*, 2020. 2
- [44] Dmitry Ulyanov, Andrea Vedaldi, and Victor Lempitsky. Instance normalization: The missing ingredient for fast stylization. *arXiv preprint arXiv:1607.08022*, 2016. 5
- [45] Rahul Rama Varior, Mrinal Haloi, and Gang Wang. Gated siamese convolutional neural network architecture for human re-identification. In *European conference on computer vision*, pages 791–808. Springer, 2016. 2
- [46] Rahul Rama Varior, Bing Shuai, Jiwen Lu, Dong Xu, and Gang Wang. A siamese long short-term memory architecture for human re-identification. In *European conference on computer vision*, pages 135–153. Springer, 2016. 2
- [47] C. Wah, S. Branson, P. Welinder, P. Perona, and S. Belongie. The Caltech-UCSD Birds-200-2011 Dataset. Technical Report CNS-TR-2011-001, California Institute of Technology, 2011. 6
- [48] Zhihao Wang, Jian Chen, and Steven CH Hoi. Deep learning for image super-resolution: A survey. *IEEE transactions on pattern analysis and machine intelligence*, 43(10):3365–3387, 2020. 1
- [49] Jason Weston, Sumit Chopra, and Antoine Bordes. Memory networks. In *International Conference on Learning Representations*, 2015. 2
- [50] Tao Xu, Pengchuan Zhang, Qiuyuan Huang, Han Zhang, Zhe Gan, Xiaolei Huang, and Xiaodong He. Attngan: Fine-grained text to image generation with attentional generative adversarial networks. In *Proceedings of the IEEE conference on computer vision and pattern recognition*, pages 1316–1324, 2018. 1, 2, 3, 5, 6, 7, 8
- [51] Guojun Yin, Bin Liu, Lu Sheng, Nenghai Yu, Xiaogang Wang, and Jing Shao. Semantics disentangling for text-to-image generation. In *Proceedings of the IEEE Conference on Computer Vision and Pattern Recognition*, pages 2327–2336, 2019. 1, 2, 6, 7, 8
- [52] Fangchao Yu, Li Wang, Xianjin Fang, and Youwen Zhang. The defense of adversarial example with conditional generative adversarial networks. *Security and Communication Networks*, 2020, 2020. 2
- [53] Mingkuan Yuan and Yuxin Peng. Ckd: Cross-task knowledge distillation for text-to-image synthesis. *IEEE Transactions on Multimedia*, 2019. 1
- [54] Han Zhang, Ian Goodfellow, Dimitris Metaxas, and Augustus Odena. Self-attention generative adversarial networks. In *International conference on machine learning*, pages 7354–7363. PMLR, 2019. 2, 3
- [55] Han Zhang, Jing Yu Koh, Jason Baldridge, Honglak Lee, and Yinfei Yang. Cross-modal contrastive learning for text-to-image generation. In *Proceedings of the IEEE/CVF Conference on Computer Vision and Pattern Recognition*, pages 833–842, 2021. 6, 7
- [56] Han Zhang, Tao Xu, Hongsheng Li, Shaoting Zhang, Xiaogang Wang, Xiaolei Huang, and Dimitris N Metaxas. Stackgan: Text to photo-realistic image synthesis with stacked generative adversarial networks. In *Proceedings of the IEEE international conference on computer vision*, pages 5907–5915, 2017. 1, 2, 3, 5, 6, 7, 8

- [57] Han Zhang, Tao Xu, Hongsheng Li, Shaoting Zhang, Xiaogang Wang, Xiaolei Huang, and Dimitris N Metaxas. Stack-gan++: Realistic image synthesis with stacked generative adversarial networks. *IEEE TPAMI*, 41(8):1947–1962, 2018. [1](#), [2](#), [3](#), [5](#), [6](#), [7](#)
- [58] Zhenxing Zhang and Lambert Schomaker. Dtgan: Dual attention generative adversarial networks for text-to-image generation. In *2021 International Joint Conference on Neural Networks (IJCNN)*, pages 1–8. IEEE, 2021. [6](#)
- [59] Jun-Yan Zhu, Taesung Park, Phillip Isola, and Alexei A Efros. Unpaired image-to-image translation using cycle-consistent adversarial networks. In *Proceedings of the IEEE international conference on computer vision*, pages 2223–2232, 2017. [2](#)
- [60] Minfeng Zhu, Pingbo Pan, Wei Chen, and Yi Yang. Dm-gan: Dynamic memory generative adversarial networks for text-to-image synthesis. In *Proceedings of the IEEE Conference on Computer Vision and Pattern Recognition*, pages 5802–5810, 2019. [1](#), [2](#), [6](#), [7](#), [8](#)